J Pharmacol Sci **119**, 251 – 259 (2012)

Journal of Pharmacological Sciences

Full Paper

Sulfaphenazole Attenuates Myocardial Cell Apoptosis Accompanied With Cardiac Ischemia–Reperfusion by Suppressing the Expression of BimEL and Noxa

Yasuhiro Ishihara[1,2,*] and Norio Shimamoto[2]

[1]*Graduate School of Integrated Arts and Sciences, Hiroshima University, Higashi-Hiroshima, Hiroshima 739-8521, Japan*
[2]*Laboratory of Pharmacology, Kagawa School of Pharmaceutical Sciences, Tokushima Bunri University, Sanuki, Kagawa 769-2193, Japan*

Received March 29, 2012; Accepted May 16, 2012

Abstract. We previously reported the administration of a potent cytochrome P450 inhibitor, sulfaphenazole (SPZ), to suppress oxidative stress and the extension of myocardial infarct size in a rat model of cardiac ischemia–reperfusion (I/R). The aim of this study was to investigate the effects of SPZ on the myocardial cell apoptosis induced by I/R in rats. I/R injury was evoked by ligation of the left anterior descending coronary artery for 1 h, followed by reperfusion for 3 h. TUNEL-positive nuclei were detected and nucleosomal DNA fragmentation was observed 3 h after reperfusion. The administration of SPZ largely suppressed the cardiac DNA fragmentation induced by I/R. A pan-caspase inhibitor, z-VAD-fmk, had no effect on DNA fragmentation. Caspase-3/7 was not activated 3 h after reperfusion. Decreases in the mitochondrial membrane potential and cytochrome *c* release from the mitochondria to cytosol were detected 3 h after reperfusion. The expression levels of BimEL and Noxa were elevated 3 h after reperfusion. These phenomena were suppressed by the administration of SPZ. Taken together, treatment with SPZ could attenuate the myocardial cell apoptosis accompanied with I/R by inhibiting the mitochondrial dysfunction due to decreases in the expression of BimEL and Noxa.

Keywords: heart, ischemia–reperfusion injury, apoptosis, mitochondria, sulfaphenazole

Introduction

Once the myocardium undergoes severe ischemia, restoration of blood flow is a prerequisite for myocardial salvaging. However, it may also induce deleterious changes, such as enzyme release, decreased myocardial contraction, and arrhythmias, which occur at the time of reperfusion, and are termed ischemia–reperfusion (I/R) injury (1). Cardiac I/R injury represents a clinically relevant problem associated with thrombolysis, angioplasty, and coronary bypass surgery.

For a long time, necrosis was regarded as the sole cause of cell death in myocardial infarction. However, it was recently revealed that apoptosis also plays an important role in the process of cardiomyocyte damage subsequent to myocardial infarction. Many studies have demonstrated that apoptosis was implicated in experimental I/R models (2) and furthermore, cardiac reperfusion was shown to accelerate the occurrence of apoptotic cell death in cardiomyocytes (3). Therefore, elucidating the mechanism of cardiac apoptosis induced by reperfusion is now a major research focus.

One of the major factors closely involved in the myocardial damage after reperfusion is reactive oxygen species (ROS) (4). Not only ROS *per se*, but also their oxidation products, can trigger apoptosis. It has been reported that ROS or their oxidation products directly act on mitochondria to induce the opening of the permeability transition pore, followed by the release of pro-apoptotic molecules from mitochondria (5). ROS oxidize thioredoxin proteins, which cause the release of apoptosis signal–regulating kinase 1 from thioredoxin to initiate a kinase signaling cascade, leading to apoptosis (6). Furthermore, ROS were shown to transcriptionally activate

*Corresponding author. ishiyasu@hiroshima-u.ac.jp
Published online in J-STAGE on June 28, 2012 (in advance)
doi: 10.1254/jphs.12079FP

various pro-apoptotic molecules, such as Fas and Bax, followed by the induction of apoptotic morphological changes to the cells (7, 8).

Cytochrome P450 is a monooxygenase expressed in various tissues including hearts and catalyzes the oxidation of many exogenous and endogenous compounds. Cytochrome P450 is also known to produce ROS via their catalytic cycle with or without substrate metabolism (9). Recently, it has been reported that ROS generated from cytochrome P450 play an important role in cardiac I/R injury. Granville et al. first reported the suppressive action of a potent cytochrome P450 inhibitor, sulfaphenazole (SPZ), on myocardial infarction accompanied with global I/R using a rat Langendorff preparation (10). We previously reported that intravenous administration of SPZ at the time of reperfusion reduced the myocardial infarct size and improved the cardiac function in a rat model of I/R (11). We further revealed that the suppressive effects of SPZ on myocardial infarction were brought about by the attenuation of the cardiac ROS levels derived from cytochrome P450 (12).

Khan et al. showed that SPZ-induced cardioprotection was mediated by the enhancement of nitric oxide bioavailability due to the increased expression of inducible nitric oxide synthase in a rat Langendorff preparation (13). Huang et al. demonstrated that protein kinase C activation and subsequent autophagy were involved in the cardioprotection induced by SPZ, also using Langendorff preparations (14). However, there is currently no evidence of how SPZ affects the myocardial cell apoptosis induced by I/R. The aim of this study was to investigate the action of SPZ on the myocardial cell apoptosis induced by I/R using an in vivo rat model of cardiac I/R. In this study, we first demonstrate the inhibitory action of SPZ on myocardial cell apoptosis during reperfusion, and then examine the mechanism(s) underlying the inhibitory effects of SPZ on myocardial cell apoptosis.

Materials and Methods

Materials

SPZ was obtained from Sigma-Aldrich (St. Louis, MO, USA). The z-VAD-fmk was purchased from Biomol International (Plymouth Meeting, PA, USA). Safranin O was obtained from Thermo Fisher Scientific (Geel, Belgium). All other chemicals were obtained from Sigma-Aldrich or Wako Pure Industries, Limited (Osaka) and were of reagent grade.

Animals

All procedures performed on animals were in accordance with the Fundamental Guidelines for Proper Conduct of Animal Experiment and Related Activities in Academic Research Institutions under the jurisdiction of the Ministry of Education, Culture, Sports, Science, and Technology, Japan and the Animal Care and Use Committee of Tokushima Bunri University, Kagawa, Japan.

Male Wistar rats (250 – 350 g) obtained from Nippon CLEA (Osaka) were maintained in a temperature-controlled animal house with a 12-h light–dark cycle. The rats had free access to food and water. The rats underwent experimentation only after acclimation for 7 – 14 days in the animal facility.

Protocol for the induction of myocardial I/R and isolation of the ischemic region from the non-ischemic region

The induction of myocardial I/R was performed as previously reported (11). Briefly, rats were anesthetized with pentobarbital sodium (40 mg/kg i.p.). Under artificial ventilation, a left thoracotomy at the fourth costal space was performed, and the left anterior descending coronary artery (LAD) was occluded for 1 h by tightening a snare of thread. The LAD was reperfused by untying the thread. After the 3-h reperfusion period, the LAD was re-occluded at the same position, and the heart was excised. Evans blue dye (0.1%) was injected into the aorta to visualize the non-ischemic region.

Experimental protocol

The LAD was occluded for 1 h and then reperfused for 3 h. SPZ (30 mg/kg) and z-VAD-fmk (3 mg/kg) were administered into the femoral vein at the beginning of reperfusion. SPZ was dissolved in 0.1 M sodium hydroxide at 20 mg/mL and then injected. The z-VAD-fmk was dissolved in dimethyl sulfoxide (20 mg/mL), and 3 mg/kg of z-VAD-fmk in 500 μL of saline was injected. The above concentrations of sodium hydroxide and dimethyl sulfoxide used as vehicles showed no effect on the blood pressure, heart rate, and rate–pressure product (Table 1).

Detection of DNA fragmentation

The TUNEL assay was performed using the DeadEnd™ Fluorometric TUNEL System (Promega, Madison, WI, USA) according to our previous report (15). Briefly, frozen sections of the heart were fixed, and then fluorescein-12-dUTP was catalytically incorporated into the fragmented DNA at the 3′-OH by terminal deoxynucleotidyl transferase. The fluorescein-12-dUTP–labeled DNA was visualized directly using a BX51WI fluorescence microscope (Olympus, Tokyo). TUNEL-positive cells were identified from fluorographs of at least 300 nuclei.

For the detection of nucleosomal DNA fragmentation,

Table 1. Effects of vehicles on hemodynamic parameters

	Untreated	Sodium hydroxide	Dimethyl sulfoxide
Mean blood pressure (mmHg)	101 ± 5	106 ± 4	103 ± 7
Heart rate (beats/min)	383 ± 8	372 ± 10	372 ± 7
Rate–pressure product (mmHg × beats/min × 10^{-3})	56.9 ± 2.6	53.2 ± 2.0	55.8 ± 2.2

Sodium hydroxide or dimethyl sulfoxide was administrated into the femoral vein, and then the mean blood pressure was measured with a fluid-filled catheter connected to a pressure transducer (DH-100; Nihon Kohden, Tokyo) and inserted into the right carotid artery. The rate–pressure product was calculated from the heart rate and left ventricular systolic pressure that were monitored using a high-fidelity catheter-tip micro-manometer (2F; Millar Instruments, Inc., Houston, TX, USA), inserted into the right carotid artery to the left ventricle. Values are the mean ± S.E.M. of 5 separate experiments.

an Apoptosis DNA Ladder Kit (Wako) was used (16). The extracted DNA was separated by 1.5% agarose gel electrophoresis, stained with SYBR Green I, and then visualized under ultraviolet light.

Measurement of caspase-3/7 activity

Myocardial tissue specimens were frozen and homogenized in the lysis buffer (25 mM HEPES-NaOH, pH 7.5, 0.1% TritonX-100, 5 mM $MgCl_2$, 2 mM DTT) and centrifuged at 10,000 × *g* for 20 min at 4°C. The caspase-3/7 activity of the supernatant was determined using an Apo-ONE Homogeneous Caspase-3/7 Assay kit (Promega) according to the manufacturer's instructions.

Immunoblotting

Myocardial tissue specimens were frozen and then lysed in RIPA buffer (25 mM Tris-HCl, pH 7.6, 150 mM NaCl, 1% NP-40, 1% sodium deoxycholate and 0.1% SDS). Equal amounts of protein were loaded and separated by SDS-PAGE using a 10% or 12% (w/v) polyacrylamide gel and then transferred onto a polyvinylidene difluoride membrane. The blocked membranes were incubated with primary antibodies of anti-caspase-3 (1/1,000; BD Biosciences, Franklin Lakes, NJ, USA), anti-cytochrome *c* (1/1,000; BD Biosciences), anti-COXIV (1/2,000; Molecular Probe, Eugene, OR, USA), anti-Bim (1/1,000; Cell Signaling Technology, Beverly, MA, USA) or anti-Noxa (1/1,000; Imgenex Corporation, San Diego, CA, USA). The membranes were incubated with an Alexa680-conjugated secondary antibody (Invitrogen) and then visualized. The band intensity was quantified using Image J software program (NIH, Bethesda, MD, USA).

Isolation of the cytosolic fraction and mitochondria

The fractionation of myocardial cytosol by a multistep centrifugation method was described previously (15). Briefly, the rat myocardium was homogenized in the buffer [50 mM Tris-HCl, pH 7.4, 154 mM KCl, 1 mM EDTA, and 1 mM DTT containing aprotease inhibitor cocktail (Nacalai, Kyoto)] and centrifuged at 10,000 × *g* for 20 min at 4°C. The supernatant was re-centrifuged at 100,000 × *g* for 60 min at 4°C. The resulting supernatant was then used as the cytosolic fraction for cytochrome *c* detection.

Rat myocardial mitochondria were isolated according to the report by Hopper et al (17). The myocardial tissues (0.5 g pieces) were minced in 2 mL of isolation buffer (0.28 M sucrose, 10 mM HEPES, pH 7.2, and 0.2 mM EDTA). Trypsin (0.25 mg) was then added, and the tissue was incubated for 15 min at 4°C. The digestion was stopped by adding 20 mL of isolation buffer with 1 mg/mL bovine serum albumin and 1 mg of trypsin inhibitor. The tissue was homogenized and then centrifuged at 600 × *g* for 10 min at 4°C, and the supernatant was centrifuged at 8,000 × *g* for 15 min. The pellet was resuspended in the experimental buffer (137 mM KCl, 10 mM HEPES, pH 7.2, and 2.5 mM $MgCl_2$) and stored on ice. This mitochondria-rich fraction was used for the measurement of the membrane potential and the detection of cytochrome *c*.

Measurement of the mitochondrial membrane potential

The membrane potential of intact myocardial mitochondria was estimated by the safranin O method (18). The accumulation of safranin O in the mitochondria is driven by the mitochondrial membrane potential, and results in a decrease in fluorescence. Depolarization results in the release of safranin O from the mitochondria and a subsequent increase in fluorescence. Freshly isolated mitochondria (0.5 mg protein) were suspended in 3 mL of the standard reaction medium (150 mM sucrose, 5 mM Tris-HCl, pH 7.4, 50 mM KCl, 10 μM EGTA, and 1 mM Na_3PO_4) in the presence of 8 μM safranin O. An increase in membrane potential was induced by the addition of 2 mM pyruvate and 5 mM malate as substrates. The changes in safranin O fluorescence were recorded using an F-7000 spectrofluorometer (Hitachi High-Technologies Corporation, Tokyo) operating at wavelengths of 525 nm for excitation and 575 nm for

emission.

mRNA isolation and semi-quantitative reverse transcription–polymerase chain reaction (RT-PCR)

Total RNA extraction from cardiac tissue was performed using an RNAiso Plus (Takara Bio, Inc., Kusatsu). First-strand cDNA was synthesized from 1 μg of total RNA using a RNA PCR Kit (AMV) Ver. 3.0 (Takara Bio, Inc.). For the PCR analysis, cDNA was amplified by Blend Taq Plus (Toyobo, Osaka). The primer pairs used in this study were listed in Table 2. The amplified products were separated by electrophoresis on 1.5% agarose gels. The band was visualized by ethidium bromide staining and then quantified by densitometry (Image J software program). The mRNA levels of Bcl-2 family members were divided by those of β-actin to calculate the relative mRNA levels.

Determination of the protein content

The protein content was determined according to the BCA method (BCA Protein Assay Reagent Kit; Pierce, Rockford, IL, USA) using bovine serum albumin as a standard.

Statistical analyses

All data are expressed as the means ± standard error (S.E.M.). The data were compared using Student's *t*-test with Holm's corrections for multiple comparisons. Probability (P) values < 0.05 were considered to be statistically significant.

Results

The induction of myocardial ischemia by LAD occlusion was ascertained by ST-segment elevation on an electrocardiograph (data not shown). The area at risk did not differ between groups (data not shown).

Although TUNEL-positive nuclei were rarely observed in the sham-treated group, there were approximately 7.8% TUNEL-positive nuclei in the ischemic region 3 h after reperfusion in the I/R group (Fig. 1: A and B). The administration of SPZ (30 mg/kg, i.v.) significantly decreased the number of TUNEL-positive nuclei 3 h after reperfusion (Fig. 1: A and B). There was almost no TUNEL-positive nucleus in the non-ischemic region in all groups (data not shown).

We next evaluated nucleosomal DNA fragmentation by agarose gel electrophoresis of the DNA extracted from the ischemic regions. Nucleosomal DNA fragmentation was observed in the ischemic region of the I/R group (Fig. 1C). The administration of SPZ clearly suppressed the nucleosomal DNA fragmentation that was accompanied with reperfusion (Fig. 1C). These results indicate that the myocardial cell apoptosis accompanied with cardiac I/R is suppressed by the administration of SPZ at the beginning of reperfusion.

The caspase family plays a fundamental role in apoptosis. Among all caspases, caspase-3 is one of the key executors of apoptosis, being either partially or totally responsible for the proteolytic cleavage of many essential proteins, followed by apoptotic morphological changes (19). Therefore, we evaluated the involvement of caspases in the myocardial cell apoptosis. Treatment with a pan-caspase inhibitor, z-VAD-fmk, showed no change in the number of TUNEL-positive nuclei or the nucleosomal DNA fragmentation induced by I/R (Fig. 2: A and B). Caspase-3/7 was not activated (Fig. 2C), and caspase-3 was not processed in the ischemic region 3 h after reperfusion (Fig. 2D), clearly indicating that the myocardial cell apoptosis elicited by I/R is independent of the cas-

Table 2. Primers used in this study

Target	Forward Primer (5′-3′)	Reverse Primer (5′-3′)
Bad	AGGACTTATCAGCCGAAGCAG	TTTCCTAAGGCCTCGAAAGAC
Bak	GTCAGGCAGGTGACAAGTGAG	TTAGTCCAGGCAGTCATGTGG
Bax	AGAGGCAGCGGCAGTGAT	AGACACAGTCCAAGGCAGCAG
Bid	GGTTCCCTGGACTCTGAGC	AGCTTCACAATTCTTGCCGTA
BimEL	GTAATCCCGACGGCGAAGG	CAGTGCCTTCTCCAGACCAG
BipN3	AAGCTGCCCTGCTACCTCTC	ACAGAATTCCTTTGGGGAAAA
Noxa	GGATCTAAGTCCCCTGTACGC	TTTCCCTCTCATCACAGTCCA
Puma	TGGGTGCACTGATGGAGATA	AACCTATGCAATGGGATGGA
Bcl-2	GCGAAGTGCTATTGGTACCTG	ATATTTGTTTGGGGCAGGTCT
Bcl-xL	GACTGGTTGAGCCCATCTCTA	GTGAGTGGACGGTCAGTGTCT
β-Actin	TTCAACACCCCAGCCATGTA	TGATCCACATCTGCTGGAAG

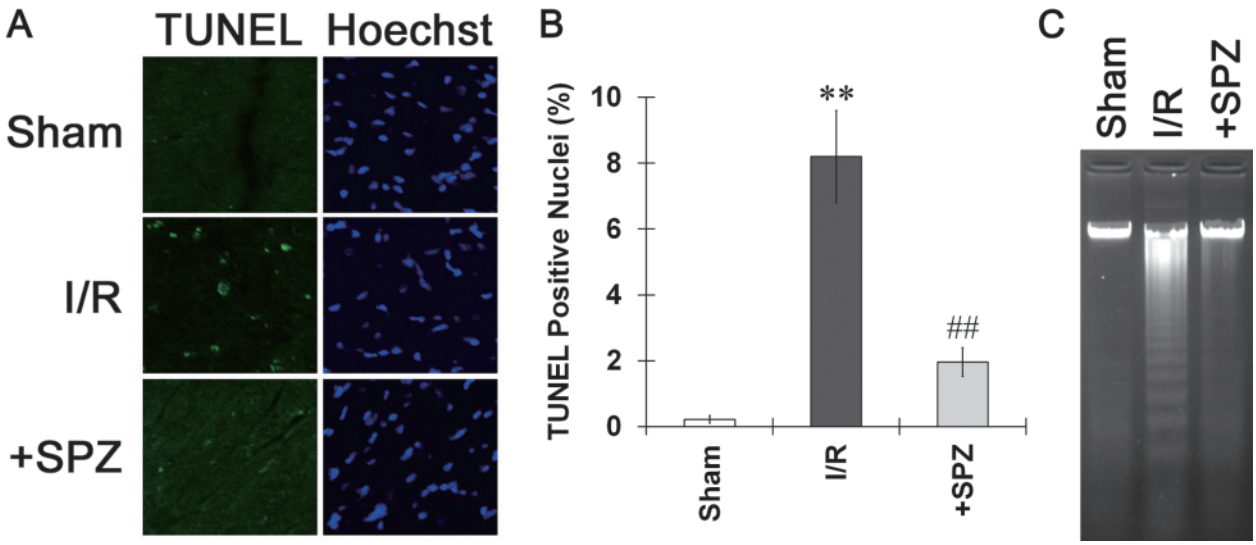

Fig. 1. Suppression of nucleosomal DNA fragmentation induced by I/R injury by the administration of SPZ. The LAD was occluded for 1 h and reperfused for 3 h. SPZ (30 mg/kg i.v.) was administered into the femoral vein at the beginning of reperfusion. The heart was excised, followed by visualization of the area at risk by injection of Evans blue dye. A, B) Frozen sections of the area at risk were prepared, and then DNA fragmentation was evaluated by TUNEL staining. A) Representative microscopic images of the TUNEL-stained tissues. B) The rate of nuclei with DNA fragmentation was calculated. The values are the means ± S.E.M. of 5 separate experiments. The data were analyzed by Student's *t*-test with Holm's corrections for multiple comparisons. $^{**}P < 0.01$ vs. the sham group, $^{\#\#}P < 0.01$ vs. the I/R group. C) DNA was extracted and then electrophoresed to evaluate nucleosomal DNA fragmentation. The results are representative of 3 independent experiments.

pase cascade under our experimental conditions.

It is well known that the mitochondrial permeability transition pore opening at the beginning of reperfusion causes a collapse of the mitochondrial membrane potential (20). Thus, we examined the involvement of the mitochondria in myocardial cell apoptosis. In the presence of the respiratory substrates pyruvate and malate, safranin O was accumulated in the mitochondria by negative membrane potential, which decreased the fluorescence intensity. The addition of Ca^{2+} to the mitochondria resulted in a transient depolarization due to electrophoretic Ca^{2+} uptake by the uniporter. Mitochondria from the I/R group built up a lower potential compared with the sham group and exhibited a higher sensitivity to Ca^{2+} addition (Fig. 3). Mitochondria isolated from the I/R+SPZ group exhibited similar changes in the mitochondrial membrane potential to those of the sham group (Fig. 3), thus indicating the protective effects of SPZ on the mitochondrial permeability transition pore opening induced by I/R. Furthermore, cytochrome *c* was not detected in the cytosolic fraction of the cardiomyocytes in the sham-treated group, while cytochrome *c* release from the mitochondria to cytosol was observed in the I/R group (Fig. 4: A – C). The administration of SPZ suppressed the cytochrome *c* release to the cytosol induced by I/R (Fig. 4: A – C). These data suggest that SPZ suppresses the mitochondrial permeability transition to attenuate the myocardial cell apoptosis induced by I/R.

Bcl-2 family proteins are closely involved in the mitochondrial types of apoptosis. It has been reported that the levels of the pro-apoptotic family are increased during apoptosis, whereas the expression of the anti-apoptotic Bcl-2 family is down-regulated (21, 22). Therefore, we examined the contribution of Bcl-2 family members to the myocardial cell apoptosis induced by I/R. The mRNA levels for ten of the Bcl-2 family members, including eight pro-apoptotic members (Bad, Bak, Bax, Bid, BimEL, BipN3, Noxa, and Puma) and two anti-apoptotic member (Bcl-2 and Bcl-xL), were evaluated 3 h after reperfusion using semiquantitative RT-PCR. The mRNA levels of Bad, Bak, Bid, BipN3, Puma, Bcl-2, and Bcl-xL showed no change, but those of Bax decreased in the ischemic region 3 h after reperfusion (Fig. 5: A and B). Interestingly, the BimEL and Noxa mRNA levels largely increased 3 h after reperfusion (Fig. 5A). The administration of SPZ suppressed the mRNA expression of BimEL and Noxa induced by I/R (Fig. 6: A – C). In addition, the expression levels of the BimEL and Noxa proteins increased in the ischemic region 3 h after reperfusion compared with the sham-treated group, and the administration of SPZ decreased the protein levels of BimEL and Noxa induced by I/R (Fig. 6: D – F).

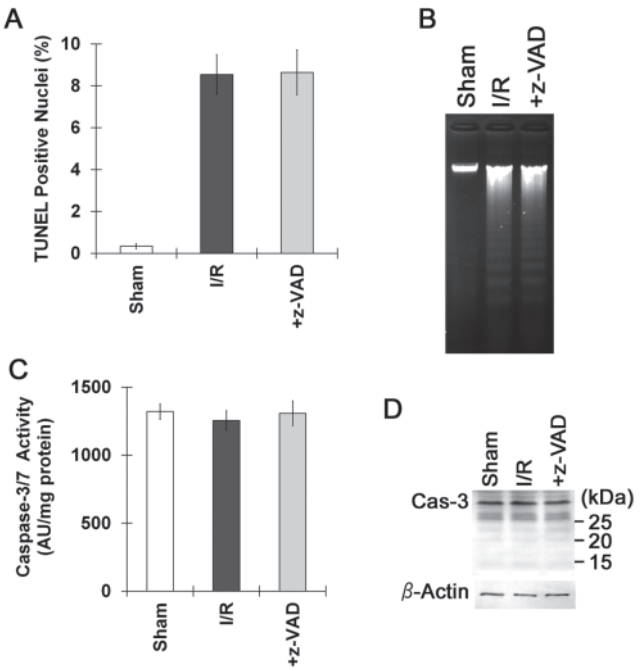

Fig. 2. The caspase-independency of the myocardial cell apoptosis induced by I/R. The LAD was occluded for 1 h and reperfused for 3 h. The z-VAD-fmk (3 mg/kg, i.v.) was administered into the femoral vein at the beginning of reperfusion. The heart was excised, followed by visualization of the area at risk by injection of Evans blue dye. A) The rate of nuclei with DNA fragmentation in the ischemic regions was measured by TUNEL staining. The values are the means ± S.E.M. of 5 separate experiments. B) DNA was extracted from the ischemic regions and then electrophoresed to evaluate nucleosomal DNA fragmentation. The results are representative of 3 independent experiments. C) Myocardial tissue of the ischemic regions was lysed and then the caspase-3/7 activity was measured. The values are the means ± S.E.M. of 4 separate experiments. D) Caspase-3 (Cas-3) processing was evaluated by immunoblotting. The results are representative of 3 independent experiments.

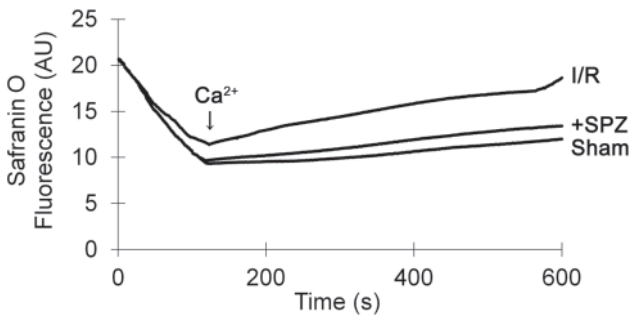

Fig. 3. The mitochondrial dysfunction that accompanied I/R was suppressed by the administration of SPZ. The LAD was occluded for 1 h and reperfused for 3 h. SPZ (30 mg/kg, i.v.) was administered into the femoral vein at the beginning of reperfusion. The heart was excised, followed by visualization of the area at risk by injection of Evans blue dye. Mitochondria were isolated from the area at risk, and then incubated in the presence of 8 μM safranin O and 30 μM Ca^{2+}. Changes in fluorescence derived from safranin O were monitored for 10 min. The results are representative of 5 independent experiments.

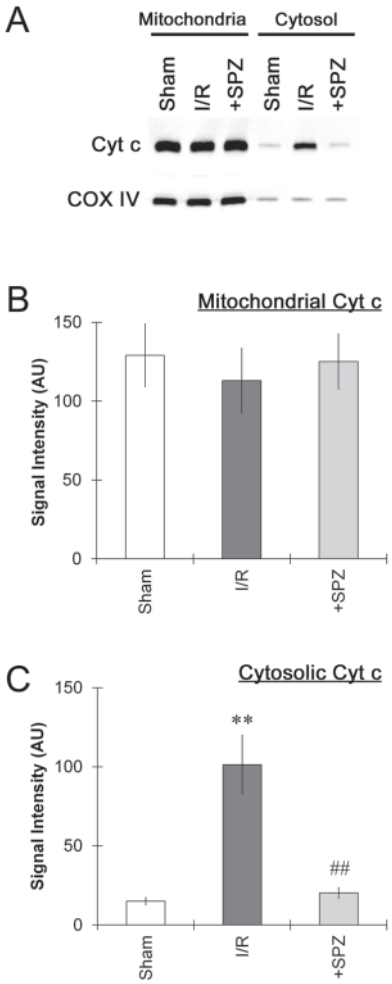

Fig. 4. Attenuation of the cytochrome *c* release from the mitochondria to the cytosol after cardiac I/R by administration of SPZ. The LAD was occluded for 1 h and reperfused for 3 h. SPZ (30 mg/kg i.v.) was administered into the femoral vein at the beginning of reperfusion. The heart was excised, followed by visualization of the area at risk by injection of Evans blue dye. The myocardial tissues of the area at risk were fractionated into mitochondrial and cytosolic fractions. Cytochrome *c* (Cyt c) was detected in the mitochondrial and cytosolic fractions by immunoblotting. COX IV is a marker of the mitochondria. A) Representative images of immunoblotting. B, C) The band intensity was measured using the Image J software program. The values are the means ± S.E.M. of 3 separate experiments. The data were analyzed by Student's *t*-test with Holm's corrections for multiple comparisons. $^{**}P < 0.01$ vs. the sham group, $^{\#\#}P < 0.01$ vs. the I/R group.

Discussion

For a long time, necrosis was regarded as the sole cause of cell death in myocardial I/R injury. However, recent studies indicate that apoptosis also plays an important role in the process of cardiomyocyte damage subsequent to myocardial infarction, and thus, the

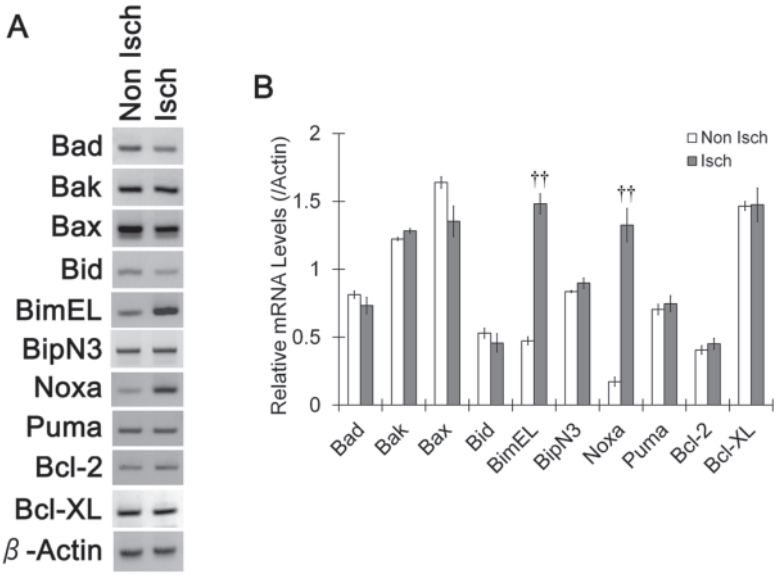

Fig. 5. Increases in the mRNA expression of BimEL and Noxa in the ischemic region of rat heart after reperfusion. The LAD was occluded for 1 h and reperfused for 3 h. The heart was excised, followed by visualization of the area at risk by injection of Evans blue dye. Total RNA was extracted from the ischemic (Isch) and non-ischemic (Non Isch) regions, and the mRNA expression level of Bcl-2 family members was evaluated by semi-quantitative RT-PCR. A) Representative images of DNA electrophoresis. B) The band was quantified, and then the mRNA levels of Bcl-2 family members were divided by those of β-actin to calculate the relative mRNA levels. The values are the means ± S.E.M. of 4 separate experiments. The data were analyzed by Student's *t*-test. $^{\dagger\dagger}P < 0.01$ vs. non-ischemic regions.

mechanism(s) underlying the cardiac apoptosis have been explored. Under our experimental conditions, myocardial cell apoptosis accompanied with nucleosomal DNA fragmentation was induced in a rat model of I/R. This apoptosis occurred in a caspase-independent manner and was executed via the mitochondrial pathway. In addition, because the expression of BimEL and Noxa was elevated in the ischemic region, these proteins are considered to contribute to the execution of apoptosis after cardiac reperfusion.

Caspase family proteins, especially caspase-3, are known as major apoptosis executors. Pro-caspases are proteolytically cleaved and activated to form active caspases. The activated caspases then cleave various intracellular proteins, such as actin, nuclear lamin and inhibitor of caspase-activated DNase, followed by the induction of apoptotic features, cell shrinkage, chromatin condensation, and DNA fragmentation in the cell. However, caspase-independent apoptosis has been recently reported (23), and therefore, all types of apoptosis are not induced by the action of caspases. In this study, while apoptosis accompanied with nucleosomal DNA fragmentation was detected, the caspase-3 activity was not elevated, and treatment with a pan-caspase inhibitor, z-VAD-fmk, showed no effect on apoptosis. Therefore, caspases are not involved in myocardial cell apoptosis under our experimental conditions.

ROS are reported to have dual actions for caspases; ROS activate caspases, leading to caspase-dependent apoptosis (24), but ROS also oxidize the thiol groups of either pro-caspase-3 or caspase-3, which causes a loss of caspase-3 proteolytic activity and induces caspase-independent apoptosis (25, 26). Under our experimental conditions, the ROS were generated during the early period of reperfusion, and the myocardial tissue was highly oxidized (11). Therefore, in this study, caspases were considered not to be activated under the severe oxidative conditions during reperfusion.

The Bcl-2 family has an important role in apoptosis under various conditions. The apoptosis induced by the Bcl-2 family protein(s) is considered to occur in the following manner: Bax/Bak oligomerize as a result of apoptotic stimuli and form a permeable pore in the outer mitochondrial membrane, followed by the release of proapoptotic proteins such as cytochrome *c*, apoptosis-inducing factor, and/or endonuclease G from the mitochondria (27, 28). Under normal conditions, Bax/Bak interacts with antiapoptotic Bcl-2 family members such as Bcl-2 and Bcl-xL to inhibit the ability of Bax/Bak to permeabilize the mitochondria. BimEL and Noxa are considered to activate the mitochondrial permeability transition mediated by Bax/Bak through two mechanisms (29): i) BimEL and Noxa bind to antiapoptotic Bcl-2 family proteins to liberate Bax/Bak, leading to the mitochondrial permeability transition, and ii) BimEL and Noxa directly activate Bax/Bak (inducing a conformational change), followed by pore formation. The detail mechanisms underlying the effects of BimEL and Noxa on the mitochondrial permeability transition and myocardial cell apoptosis will be investigated in greater detail in future studies.

SPZ has been reported to attenuate cardiac I/R injury due to enhancement of the bioavailability of nitric oxide (13) and activation of autophagy (14). However, the effects of SPZ on myocardial cell apoptosis accompanied with reperfusion were not examined. In this study, we

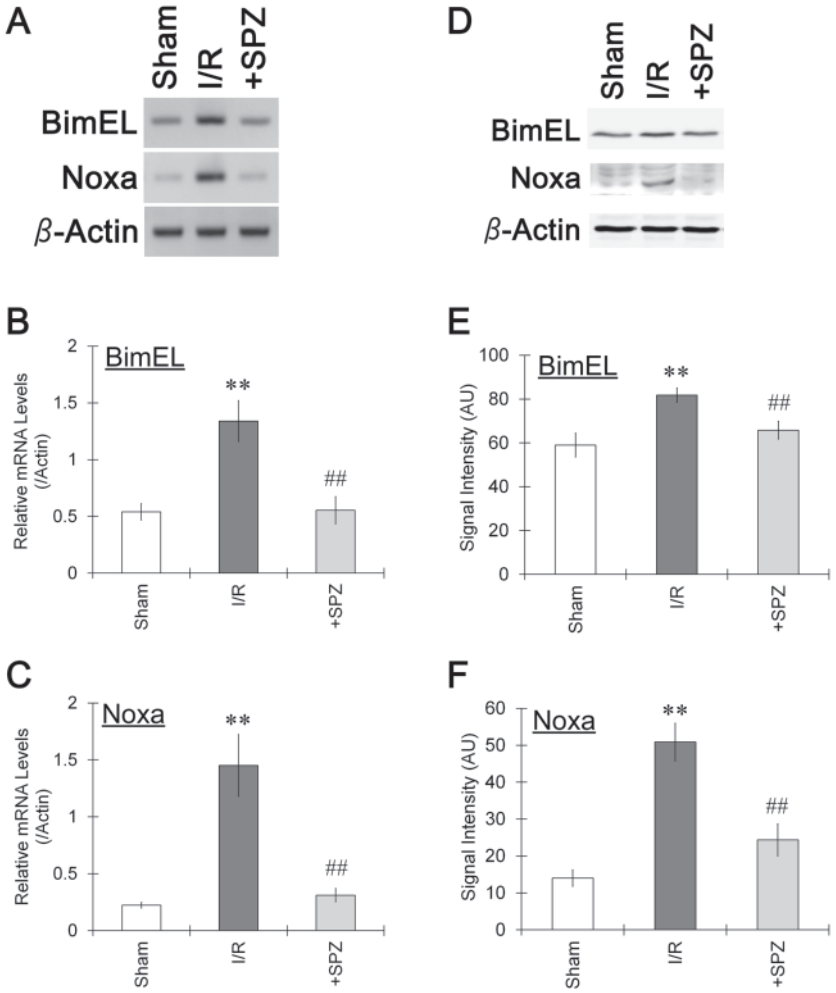

Fig. 6. Suppression of BimEL and Noxa protein expression by the administration of SPZ. The LAD was occluded for 1 h and reperfused for 3 h. SPZ (30 mg/kg, i.v.) was administered into the femoral vein at the beginning of reperfusion. The heart was excised, followed by visualization of the area at risk by injection of Evans blue dye. A – C) Total RNA was extracted from the ischemic regions, and the mRNA expression levels of BimEL, Noxa, and *β*-actin were evaluated by semi-quantitative RT-PCR. A) Representative images of DNA electrophoresis. The band intensity was measured, and the mRNA levels of BimEL (B) and Noxa (C) were divided by those of *β*-actin to calculate the relative mRNA levels. The values are the means ± S.E.M. of 4 separate experiments. The data were analyzed by Student's *t*-test with Holm's corrections for multiple comparisons. $^{**}P < 0.01$ vs. the sham group, $^{\#\#}P < 0.01$ vs. the I/R group. D – F) The myocardial tissues of the area at risk were lysed, and then the amounts of the BimEL, Noxa, and *β*-actin proteins were evaluated by immunoblotting. D) Representative images of immunoblotting. The band intensity of BimEL (E) and Noxa (F) was measured using the Image J software program. The values are the means ± S.E.M. of 4 separate experiments. The data were analyzed by Student's *t*-test with Holm's corrections for multiple comparisons. $^{**}P < 0.01$ vs. the sham group, $^{\#\#}P < 0.01$ vs. the I/R group.

revealed that SPZ suppressed the caspase-independent myocardial cell apoptosis via the mitochondrial pathway. Furthermore, the mechanism underlying the suppressive effect of SPZ on myocardial cell apoptosis was suggested to be due to the attenuation of BimEL and Noxa expression. SPZ is a potent cytochrome P450 inhibitor (30). We previously reported that SPZ suppressed cardiac reperfusion injury by inhibiting ROS production from cytochrome P450 (11, 12). We showed that BimEL expression was elevated by ROS stimuli (31). The levels of Noxa proteins are also known to be increased by ROS (32, 33). Therefore, the expression of BimEL and Noxa is considered to be induced downstream of the ROS that are generated during reperfusion, and SPZ might suppress the expression of BimEL and Noxa by attenuating the ROS production from cytochrome P450.

In conclusion, caspase-independent and mitochondria-mediated apoptosis was induced by cardiac I/R. This apoptosis was accompanied by increased expression of BimEL and Noxa. The administration of SPZ at the beginning of reperfusion suppressed not only BimEL and Noxa expression, but also the apoptosis induced by cardiac I/R. Therefore, SPZ is considered to have cardioprotective effects against I/R injury by suppressing the myocardial cell apoptosis arising due to decreases in the expression of BimEL and Noxa.

Acknowledgments

This work was supported by Grants-in-Aid for Scientific Research (to Y.I.) from the Japan Society for the Promotion of Science (JSPS), a grant from Tokushima Bunri University for Educational Reform and Collaborative Research (to Y.I.) and a Research Grant from Kagawa School of Pharmaceutical Sciences, Tokushima Bunri University for Young Scientists (to Y.I.). We are grateful to Dr. Takeshi Yamazaki, Hiroshima University for his assistance in writing the manuscript.

References

1 Opie LH. Reperfusion injury and its pharmacologic modification. Circulation. 1989;80:1049–1062.
2 Fliss H, Gattinger D. Apoptosis in ischemic and reperfused rat myocardium. Circ Res. 1996;79:949–956.
3 Haunstetter A, Izumo S. Apoptosis: basic mechanisms and impli-

cations for cardiovascular disease. Circ Res. 1998;82:1111–1129.
4 Becker LB. New concepts in reactive oxygen species and cardiovascular reperfusion physiology. Cardiovasc Res. 2004;61:461–470.
5 Weiss JN, Korge P, Honda HM, Ping P. Role of the mitochondrial permeability transition in myocardial disease. Circ Res. 2003;93:292–301.
6 Nishida K, Otsu K. The role of apoptosis signal-regulating kinase 1 in cardiomyocyte apoptosis. Antioxid Redox Signal. 2006;8:1729–1736.
7 Kalivendi SV, Konorev EA, Cunningham S, Vanamala SK, Kaji EH, Joseph J, et al. Doxorubicin activates nuclear factor of activated T-lymphocytes and Fas ligand transcription: role of mitochondrial reactive oxygen species and calcium. Biochem J. 2005;389:527–539.
8 Wang N, Minatoguchi S, Chen X, Uno Y, Arai M, Lu C, et al. Antidiabetic drug miglitol inhibits myocardial apoptosis involving decreased hydroxyl radical production and Bax expression in an ischaemia/reperfusion rabbit heart. Br J Pharmacol. 2004;142:983–990.
9 Zangar RC, Davydov DR, Verma S. Mechanisms that regulate production of reactive oxygen species by cytochrome P450. Toxicol Appl Pharmacol. 2004;199:316–331.
10 Granville DJ, Tashakkor B, Takeuchi C, Gustafsson AB, Huang C, Sayen MR, et al. Reduction of ischemia and reperfusion-induced myocardial damage by cytochrome P450 inhibitors. Proc Natl Acad Sci U S A. 2004;101:1321–1326.
11 Ishihara Y, Sekine M, Nakazawa M, Shimamoto N. Suppression of myocardial ischemia-reperfusion injury by inhibitors of cytochrome P450 in rats. Eur J Pharmacol. 2009;611:6471.
12 Ishihara Y, Sekine M, Hamaguchi A, Kobayashi Y, Harayama T, Nakazawa M, et al. Effects of sulfaphenazole derivatives on cardiac ischemia-reperfusion injury: association of cytochrome P450 activity and infarct size. J Pharmacol Sci. 2010;113:335–342.
13 Khan M, Mohan IK, Kutala VK, Kotha SR, Parinandi NL, Hamlin RL, et al. Sulfaphenazole protects heart against ischemia-reperfusion injury and cardiac dysfunction by overexpression of iNOS, leading to enhancement of nitric oxide bioavailability and tissue oxygenation. Antioxid Redox Signal. 2009;11:725–738.
14 Huang C, Liu W, Perry CN, Yitzhaki S, Lee Y, Yuan H, et al. Autophagy and protein kinase C are required for cardioprotection by sulfaphenazole. Am J Physiol Heart Circ Physiol. 2010;298:H570–H579.
15 Ishihara Y, Shimamoto N. Involvement of endonuclease G in nucleosomal DNA fragmentation under sustained endogenous oxidative stress. J Biol Chem. 2006;281:6726–6733.
16 Ishihara Y, Ito F, Shimamoto N. Increased expression of c-Fos by extracellular signal-regulated kinase activation under sustained oxidative stress elicits BimEL upregulation and hepatocyte apoptosis. FEBS J. 2011;278:1873–1881.
17 Hopper RK, Carroll S, Aponte AM, Johnson DT, French S, Shen RF, et al. Mitochondrial matrix phosphoproteome: effect of extra mitochondrial calcium. Biochemistry. 2006;45:2524–2536.
18 Akerman KE, Wikstrom MK. Safranine as a probe of the mitochondrial membrane potential. FEBS Lett. 1976;68:191–197.
19 Hattori Y, Takano K, Teramae H, Yamamoto S, Yokoo H, Matsuda N. Insights into sepsis therapeutic design based on the apoptotic death pathway. J Pharmacol Sci. 2010;114:354–365.
20 Halestrap AP, Clarke SJ, Javadov SA. Mitochondrial permeability transition pore opening during myocardial reperfusion--a target for cardioprotection. Cardiovasc Res. 2004;61:372–385.
21 Zhong H, Xin H, Wu LX, Zhu YZ. Salidroside attenuates apoptosis in ischemic cardiomyocytes: a mechanism through a mitochondria-dependent pathway. J Pharmacol Sci. 2010;114:399–408.
22 Jin HO, Park IC, An S, Lee HC, Woo SH, Hong YJ, et al. Up-regulation of Bak and Bim via JNK downstream pathway in the response to nitric oxide in human glioblastoma cells. J Cell Physiol. 2006;206:477–486.
23 Bae S, Yalamarti B, Kang PM. Role of caspase-independent apoptosis in cardiovascular diseases. Front Biosci. 2008;13:2495–2503.
24 Chen YC, Lin-Shiau SY, Lin JK. Involvement of reactive oxygen species and caspase 3 activation in arsenite-induced apoptosis. J Cell Physiol. 1998;177:324–333.
25 Ishihara Y, Shiba D, Shimamoto N. Primary hepatocyte apoptosis is unlikely to relate to caspase-3 activity under sustained endogenous oxidative stress. Free Radic Res. 2005;39:163–173.
26 Nobel CS, Burgess DH, Zhivotovsky B, Burkitt MJ, Orrenius S, Slater AF. Mechanism of dithiocarbamate inhibition of apoptosis: thiol oxidation by dithiocarbamate disulfides directly inhibits processing of the caspase-3 proenzyme. Chem Res Toxicol. 1997;10:636–643.
27 Mikhailov V, Mikhailova M, Degenhardt K, Venkatachalam MA, White E, Saikumar P. Association of Bax and Bak homo-oligomers in mitochondria. Bax requirement for Bak reorganization and cytochrome c release. J Biol Chem. 2003;278:5367–5376.
28 Narita M, Shimizu S, Ito T, Chittenden T, Lutz RJ, Matsuda H, et al. Bax interacts with the permeability transition pore to induce permeability transition and cytochrome c release in isolated mitochondria. Proc Natl Acad Sci U S A. 1998;95:14681–14686.
29 Chipuk JE, Green DR. How do BCL-2 proteins induce mitochondrial outer membrane permeabilization? Trends Cell Biol. 2008;18:157–164.
30 Melet A, Assrir N, Jean P, Pilar Lopez-Garcia M, Marques-Soares C, Jaouen M, et al. Substrate selectivity of human cytochrome P450 2C9: importance of residues 476, 365, and 114 in recognition of diclofenac and sulfaphenazole and in mechanism-based inactivation by tienilic acid. Arch Biochem Biophys. 2003;409:80–91.
31 Ishihara Y, Takeuchi K, Ito F, Shimamoto N. Dual regulation of hepatocyte apoptosis by reactive oxygen species: Increases in transcriptional expression and decreases in proteasomal degradation of BimEL. J Cell Physiol. 2011;226:1007–1016.
32 Perez-Galan P, Roue G, Villamor N, Montserrat E, Campo E, Colomer D. The proteasome inhibitor bortezomib induces apoptosis in mantle-cell lymphoma through generation of ROS and Noxa activation independent of p53 status. Blood. 2006;107:257–264.
33 Sarma SN, Kim YJ, Song M, Ryu JC. Induction of apoptosis in human leukemia cells through the production of reactive oxygen species and activation of HMOX1 and Noxa by benzene, toluene, and o-xylene. Toxicology. 2011;280:109–117.